Research Article Open Access

Yasin Ozgurluk*, Kadir Mert Doleker, Hayrettin Ahlatci, Dervis Ozkan, Abdullah Cahit Karaoglanli

The Microstructural Investigation of Vermiculite-Infiltrated Electron Beam Physical Vapor Deposition Thermal Barrier Coatings

https://doi.org/10.1515/chem-2018-0097
received January 31, 2018; accepted March 9, 2018.

Abstract: Thermal barrier coatings (TBCs) are widely used in aerospace and aviation industries for materials required to withstand severe environments such as oxidation, hot-corrosion failure and CMAS (calcia–magnesia–alumina–silica) attack or vermiculite corrosion. This is particularly apparent in vermiculite, which can penetrate sand, volcanic ash and is the most destructive damage mechanism in the TBC system. Impurities from the desert environment such as calcia–magnesia–alumina–silica (CMAS) cause degradation of TBCs. In this research, CoNiCrAlY metallic bond coatings were deposited on Inconel 718 nickel based superalloy substrates with a thickness of around 100 μm using a Cold Gas Dynamic Spray (CGDS) technique. Production of TBCs were carried out with deposition of YSZ ceramic top coating material using Electron Beam Physical Vapor Deposition (EB-PVD), with a thickness of around 200 μm. The effect of CMAS with spreading naturally-occurring mineral (vermiculite) on TBC samples were investigated using scanning electron microscopy (SEM), energy dispersive spectroscopy (EDS) analysis and X-ray diffraction (XRD). The microstructure evolution of YSZ and failure mechanism of TBC were evaluated.

***Corresponding author: Yasin Ozgurluk,** Metallurgical and Materials Engineering Department, Karabuk University, Karabuk, 78050, Turkey; Metallurgical and Materials Engineering Department, Bartin University, Bartin, 74100 Turkey, E-mail: ozgurlukyasin@gmail.com
Kadir Mert Doleker, Hayrettin Ahlatci: Metallurgical and Materials Engineering Department, Karabuk University, Karabuk, 78050, Turkey
Kadir Mert Doleker, Abdullah Cahit Karaoglanli: Metallurgical and Materials Engineering Department, Bartin University, Bartin, 74100 Turkey
Dervis Ozkan: Mechanical Engineering Department, Bartin University, Bartin, 74100 Turkey

Keywords: Calcia–Magnesia–Alumina–Silica (CMAS) attack; Thermal Barrier Coatings (TBCs); Electron Beam Physical Vapor Deposition (EB-PVD); Cold Gas Dynamic Spray (CGDS).

PACS: 81.15.Rs, 81.15.–z, 07.85.–m.

1 Introduction

Thermal barrier coatings (TBCs) are widely used in gas turbine engine parts exposed to high temperatures to increase the efficiency and reduce the fuel consumption in space and aviation industries [1-7]. TBCs provide thermal insulation on metallic parts of gas turbine engines (such as blades, valves and combustion chambers), providing significant resistance to corrosion, erosion and oxidation at high temperatures [8,9]. TBC systems consist of a superalloy metallic base, an oxidation-resistant bond coating, and a high-dielectric top coating of insulating material to provide thermal insulation [10-14]. Generally, the production of the TBC system takes place by atmospheric plasma spray (APS) and electron beam-physical vapour deposition (EB-PVD) [15,16]. The EB-PVD method is more preferred than the APS method to ensure the lifetime use of the TBCs. Because the bond strength of the EB-PVD method is higher than that of the APS method and the stress tolerance is better [17,18]. Stabilized zirconia (YSZ) with 6-8% by weight of Y_2O_3 is used as a ceramic top covering insulation material. The thermal expansion, which is very similar to the low thermal conductivity and bond coating, allows YSZ to be the most preferred ceramic top coating material in TBC systems. The excellent mechanical properties of YSZ allow the surface temperature to increase up to 1200°C. In the production of oxidation-resistant bond coatings, MCrAlY (M = Ni, Co and combinations), which have a low affinity for oxygen, are used as a metallic binding layer to protect the substrate surface from corrosion and oxidation. Recently, studies have analysed the damage of theTBC.

Table 1: Chemical composition of Inconel 718.

% Chemical Composition of Inconel-718							
Ni	**Cr**	**Nb**	**Mo**	**Ti**	**Al**	**Co**	**Si**
53.55	18.0	5.31	3.03	0.96	0.56	0.27	0.09
Cu	Mn	C	Ta	P	B	S	Fe
0.06	0.06	0.03	0.01	0.007	0.004	0.001	Balance

Table 2: Bond and top coating parameters for TBC materials.

Bond coat	**Spray pressure (bar)**	**Gas temperature (°C)**	**Working gas (slpm)**	**Spray distance (mm)**	**Gun speed (mm/s)**
CoNiCrAlY	**30**	**600**	**Helium(1000)**	**15**	**20**
Top coat	Voltage (kV)	Temperature (°C)	Vacuum (Torr)	Rotation speed (rpm)	Condensation ratio (μm/min)
YSZ	20 kV	800 ± 25 °C	$5 \times 10^{-5} - 1 \times 10^{-4}$	25	4,5

Damage mechanisms such as oxidation, thermal shock, erosion, hot corrosion and CMAS (CaO, MgO, Al_2O_3, SiO_2) effects play an active role in high temperature operating conditions in TBC systems [19,20]. Rich particles of Si, Ca, Mg and Al, such as sand and volcanic ash are seen as threats to the development of future generations and high efficiency aircraft engines operating at high temperatures [18-20]. These minerals and particles penetrate into the coating by melting and these minerals rich in silicon, which are transformed into an erosive glassy structure, solidify again when the temperature decreases and cause thermomechanical and chemical degradation of the coating. In this study, the effect of Vermiculite/CMAS on YSZ samples were investigated using several metallographic methods.

2 Experimantal

2.1 Substrate material and preparation of CoNiCrAlY bond and YSZ top coatings

Inconel 718 superalloy samples with a diameter of 25.4 mm were used as substrates. Its chemical composition is given in Table 1. CoNiCrAlY metal powders were sprayed producing metallic bond coating by using the cold gas dynamic spray (CGDS) technique with a thickness of approximately 100 μm. Then spraying bond coating, deposition of ceramic top coatings were done with a thickness about 200 μm using ZrO_2-8 wt.%Y_2O_3 (YSZ) ceramic powders by EB-PVD method. In this method, ceramic materials were used as ingots. The height of the ingots used in the coating procedure is approximately 45-55mm. The substrate material is heated to 900 ± 25°C before the coating process. The deposition parameters of the CoNiCrAlY bond coats produced by CGDS technique and the deposition parameters of the YSZ top coats, produced by EB-PVD method, are shown in Table 2.

Ethical approval: The conducted research is not related to either human or animal use.

3 Results and Discussion

3.1 Examination of Vermiculite/CMAS powder

Vermiculite/CMAS powder was ground and eliminated. Then, this powder was subjected to EDS analysis. According to the results obtained from the EDS analysis, its chemical composition contained traces of Ca and K whilst also being rich in Si, Fe, Mg and Al. EDS data is shown in Figure 1. EDS analysis was carried out on the whole picture. This mineral is a hydrous silicate and its chemical composition is showed in detail in Table 3. Vermiculite powder has a monoclinic crystal system. Its cell parameters are a (0.53nm), b (0.92nm), c (2.87nm) and space group C2/c(15).

After the chemical analysis, particle size distributions were used for obtain average particle size of CMAS powder. Malvern Mastersizer 3000 particle size analyzer was used. The average particle size distribution was found about 66.3 μm. It is shown that in Figure 2.

Table 3: Chemical composition (wt.%) of Vermiculite/CMAS powder.

Element	Weight (%) Vermiculite
O	41,5
Si	18,4
Fe	15,1
Mg	8,8
Al	8,7
K	3,6
Ca	2,2
Ti	1,7

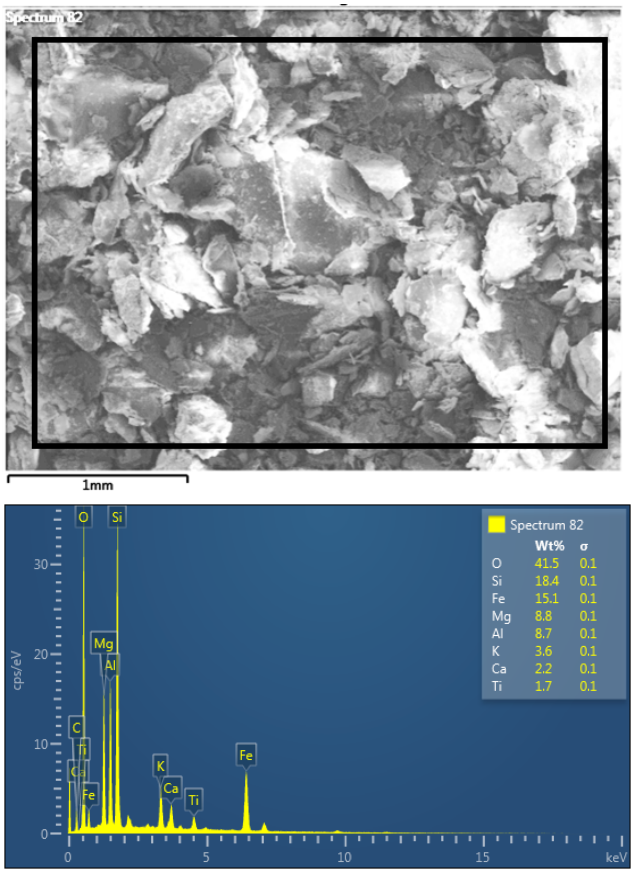

Figure 1: Chemical composition (wt.%) of Vermiculite/CMAS powder, obtained from EDS data.

According to the results obtained from the Hitachi STA 7300 DSC analysis the melting temperature of this vermiculite powder is approximately 1163°C and its glass transition temperature is about 983°C. This DSC analyzer can perform thermal analysis up to 1400°C. The DSC result is shown in Figure 3a and the XRD result of vermiculite/CMAS powder shown in Figure 3b, where it can be seen that the vermiculite/CMAS powder consist of only one phase.

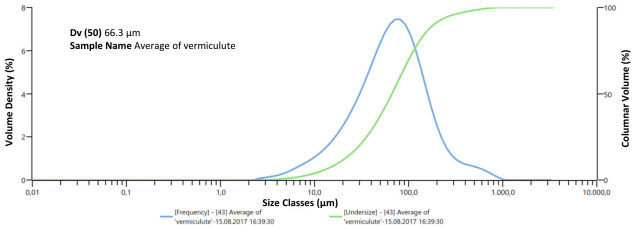

Figure 2: Particle size distributions of Vermiculite/CMAS powder.

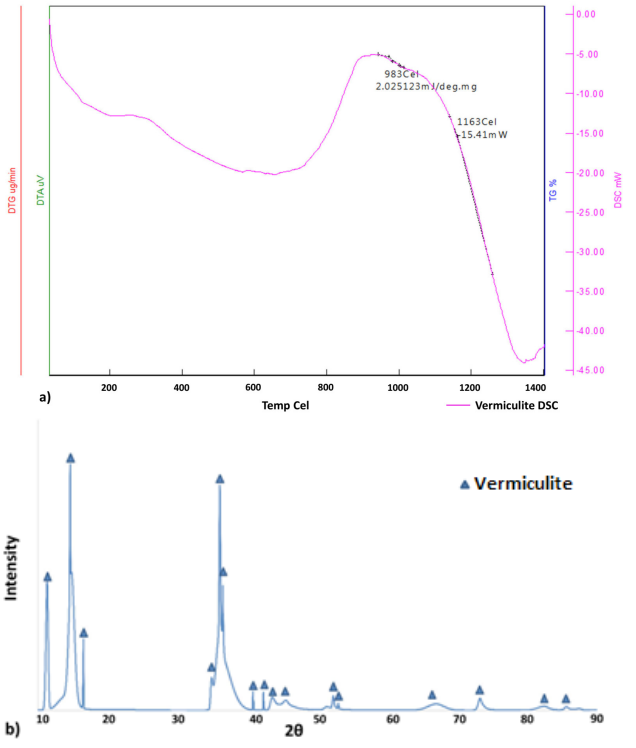

Figure 3: (a) Differential scanning calorimetry figure of Vermiculite/CMAS and (b) X-ray diffraction figure of Vermiculite/CMAS.

3.2 Vermiculite/ CMAS (CaO-MgO-Al_2O_3-SiO_2) corrosion tests

The YSZ ceramic top coated TBC samples were subjected to the CMAS corrosion tests. Vermiculite corrosion powder was sprinkled on the TBC samples in the amount of 10 mg/cm^2. TBC samples were sprinkled with vermiculite corrosion salt, placed in an electric furnace with an air atmosphere under a maximum temperature of 1200°C for 6 hours. After 2 hours of testing at 1200°C, the samples were allowed to cool down inside the furnace, and then the coatings were inspected using scanning electron microscopy (SEM). The samples were then recoated with the vermiculite salt powders. Test cycles were repeated on each sample until a 50% deterioration was observed on

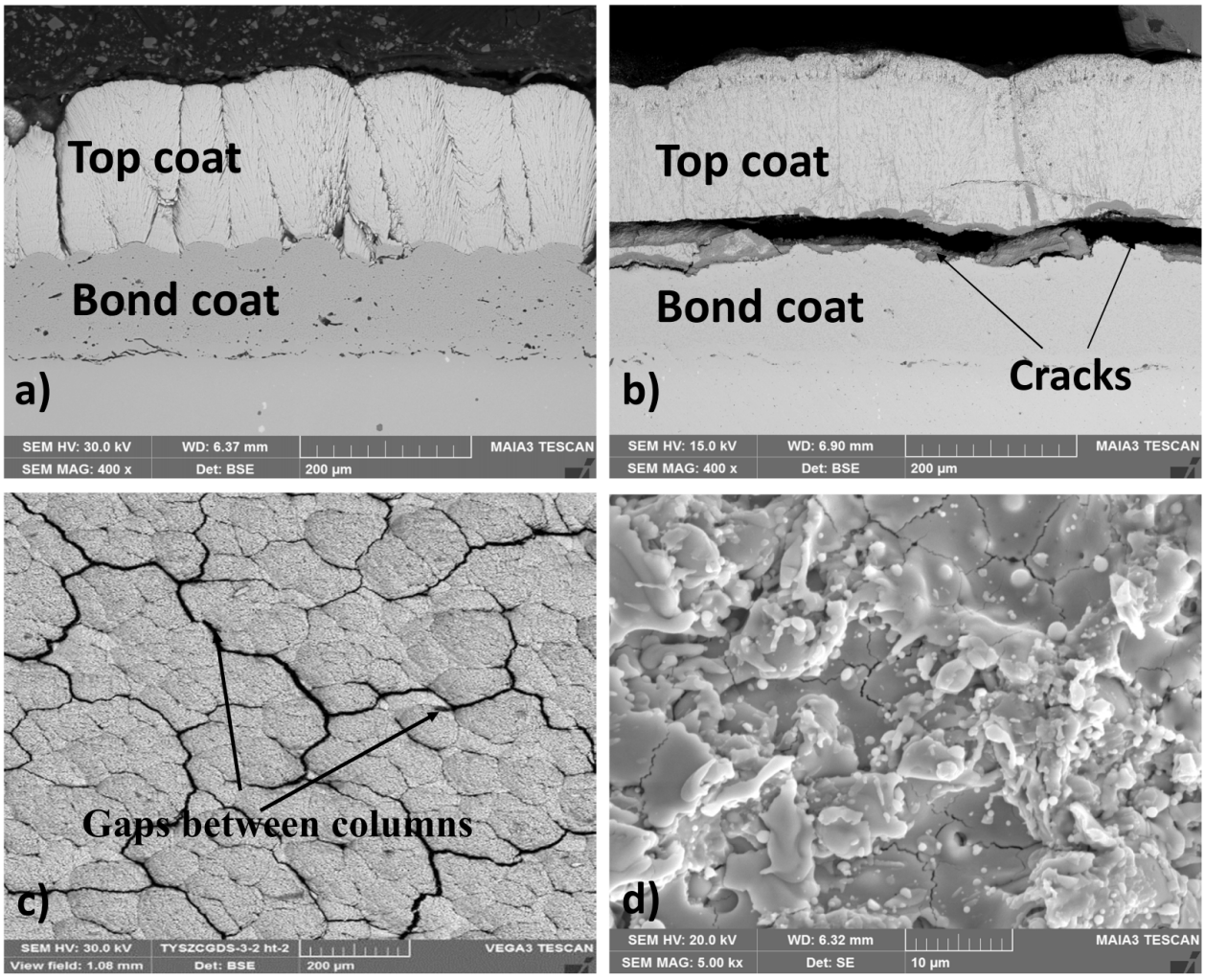

Figure 4: EB-PVD TBCs with cold sprayed CoNiCrAlY bond coat's SEM image a) cross section image before CMAS corrosion test, b) cross section image after CMAS corrosion test, c) surface image before CMAS corrosion test, d) surface image after CMAS corrosion test.

the sample surfaces. The morphology and microstructure of the as-sprayed coatings and the coatings after the vermiculite/CMAS tests were examined using field emission scanning electron microscopy.

After the Vermiculite/CMAS corrosion test, the phase structure of the colonic YSZ coating changed [17-20]. The YSZ, which was stable in the tetragonal phase, was damaged after the corrosion test. It is clear that this damage is caused by the CMAS molten powders, which have diffused into the YSZ coating. The melted glassy CMAS structure at 1200°C caused a volume increase in the coating during cooling and caused the coating to be damaged. The solubility of the melted CMAS in YSZ depends on the amount of CaO. The damage formation in YSZ also occurs by the conversion of monoclinic phase from tetragonal phase [20-22].

4 Conclusion

In this study, columnar TBCs were prepared by EB-PVD method. Used vermiculite mineral as the CMAS type corrosion powder for investigation of corrosion effect on TBC samples. The characterization of vermiculite powder and the CMAS effect of this powder at 1200°C on TBC samples were investigated. Vermiculite caused a CMAS effect on the TBC sample due to the chemical composition of the powder. The melted vermiculite interacted with the YSZ and occurred a thermo-mechanical CMAS damage to the top coating. Vermiculite penetrated into the columnar gaps on the TBC sample and the phase transformation from tetragonal Zirconia (t′-ZrO_2) to monoclinic Zirconia m-ZrO_2 occurred. After the CMAS tests, results indicated that phase transformation occur on the top coating. Test results show that phase transformation and volume

expansion (CMAS effect on TBCs) are very dangerous during the operation on turbines. In further studies, the CMAS effect generated by vermiculite will be tested on new generation TBC materials and alternative materials will be investigated for the aerospace industry.

Acknowledgments: This investigation was financially supported by Scientific Research Projects (BAP) Coordinatorship of Karabuk University with project number of KBUBAP-17-DR-259 and the Scientific and Technological Research Council of Turkey with project code of TUBITAK, 113R049. This study was carried out as a Ph.D. thesis by Yasin Ozgurluk in the Graduate School of Natural and Applied Science at the University of Karabuk, Turkey.

Conflict of interest: Authors state no conflict of interest.

References

[1] Doleker K. M. Ahlatci H. Karaoglanli A. C., Investigation of Isothermal Oxidation Behavior of Thermal Barrier Coatings (TBCs) Consisting of YSZ and Multilayered YSZ/$Gd_2Zr_2O_7$ Ceramic Layers, Oxid. Met., 2017, 88(1-2), 109-119.

[2] Song J., Zhang X., Deng C., Liu M., Zhou K., Tong X., Research of in situ modified PS-PVD thermal barrier coating against CMAS (CaO–MgO–Al_2O_3–SiO_2) corrosion. Ceram. Int., 2016, 42(2), 3163-3169.

[3] Naraparaju R., Pubbysetty P., Mechnich P., Schulz U., EB-PVD alumina (Al_2O_3) as a top coat on 7YSZ TBCs against CMAS/VA infiltration: Deposition and reaction mechanisms, J. Eur. Ceram. Soc., (in press), DOI: 10.1016/j.jeurceramsoc.2018.03.027.

[4] Chen W. R., Zhao, L. R., Review–volcanic ash and its influence on aircraft engine components. Procedia Engineering, 2015, 99, 795-803.

[5] Giehl C., Brooker R. A., Marxer H., Nowak M., An experimental simulation of volcanic ash deposition in gas turbines and implications for jet engine safety. Chem. Geol., 2017, 461, 160-170.

[6] Jang B. K., Feng F. J., Suzuta K., Tanaka H., Matsushita Y., Lee K. S., Kim H. T., Corrosion behavior of volcanic ash on sintered mullite for environmental barrier coatings. Ceram. Int., 2017, 43(2), 1880-1886.

[7] Wellman R., Whitman G. Nicholls J. R., CMAS corrosion of EB PVD TBCs: Identifying the minimum level to initiate damage, Int. J. Refract. Met. H., 2010, 28(1), 124-132.

[8] Naraparaju R., Chavez J. J. G., Schulz U., Ramana C. V., Interaction and infiltration behavior of Eyjafjallajökull, Sakurajima volcanic ashes and a synthetic CMAS containing FeO with/in EB-PVD ZrO_2-65 wt% Y_2O_3 coating at high temperature. Acta Mater., 2017, 136, 164-180.

[9] Gledhill A. D., Reddy K. M., Drexler J. M., Shinoda K., Sampath S., Padture N. P., Mitigation of damage from molten fly ash to air-plasma-sprayed thermal barrier coatings. Mater. Sci. Eng., A, 2011, 528(24), 7214-7221.

[10] Krause A. R., Li X., Padture N. P. "Interaction between ceramic powder and molten calcia-magnesia-alumino-silicate (CMAS) glass, and its implication on CMAS-resistant thermal barrier coatings." Scripta Materialia, 2016, 112, 118-122.

[11] Drexler J. M., Gledhill A. D., Shinoda K., Vasiliev A. L., Reddy K. M., Sampath S., Padture, N. P., Jet engine coatings for resisting volcanic ash damage. Adv. Mater., 2011, 23(21), 2419-2424.

[12] Mechnich P., Braue W., Volcanic Ash-Induced Decomposition of EB-PVD $Gd_2Z_{r2}O_7$ Thermal Barrier Coatings to Gd-Oxyapatite, Zircon, and Gd, Fe-Zirconolite. J. Am. Ceram. Soc., 2013, 96(6), 1958-1965.

[13] Jackson R. W., Begley M. R., Critical cooling rates to avoid transient-driven cracking in thermal barrier coating (TBC) systems, Int. J. Solids. Struct, 2014, 51(6), 1364-1374.

[14] Šulák I., Obrtlík K., Čelko L., Chráska T., Jech D., Gejdoš P., Low cycle fatigue performance of Ni-based superalloy coated with complex thermal barrier coating. Mater Charact., 2018, 139, 347-354.

[15] Kumar V., Balasubramanian K., Progress update on failure mechanisms of advanced thermal barrier coatings: A review Prog. Org. Coat., 2016, 90, 54-82.

[16] Xue Z., Ma Y., Gong S., Guo H., Impermeability of $Y_3Al_5O_{12}$ ceramic against molten glassy calcium-magnesium-alumina-silicate. Chinese J Aeronaut., (in press), DOI:/10.1016/j.cja.2018.02.007.

[17] Qureshi I. N., Shahid M., Khan A. N., Effect of Bondcoat Thickness on High Temperature Hot Corrosion of ZrO_2-$8Y_2O_3$ Thermal Barrier Coating, Acta Phys. Pol., A, 2015, 128, B314-B316.

[18] Ozgurluk Y., Doleker K. M., Karaoglanli A.C., Hot corrosion behavior of YSZ, $Gd_2Zr_2O_7$ and YSZ/$Gd_2Zr_2O_7$ thermal barrier coatings exposed to molten sulfate and vanadate salt. Appl. Surf. Sci., (in press), DOI:10.1016/j.apsusc.2017.09.47.

[19] Kirtay S., Improvement of Oxidation Resistance of Mild Steel by SiO_2-Al_2O_3 Sol Gel Coating, Acta Phys. Pol., A, 2015, 128 2-B, B90-B92.

[20] Gunen A., Micro-Abrasion Wear Behavior of Thermal-Spray-Coated Steel Tooth Drill Bits, Acta Phys. Pol., A, 2016, 130(1), 217-222.

[21] Peng H., Wang L., Guo L., Miao W., Guo H., Gong S., Degradation of EB-PVD thermal barrier coatings caused by CMAS deposits. Prog. Nat. Sci-Mater, 2012, 22(5), 461-467.

[22] Kang Y. X., et al. Defects/CMAS corrosion resistance relationship in plasma sprayed YPSZ coating, J. Alloy Compd., 2017, 694, 1320-1330.